

Noise From Voltage-Gated Ion Channels May Influence Neuronal Dynamics in the Entorhinal Cortex

JOHN A. WHITE,¹ RUBY KLINK,² ANGEL ALONSO,² AND ALAN R. KAY³

¹Department of Biomedical Engineering, Center for BioDynamics, Boston University, Boston, Massachusetts 02215;

²Department of Neurology and Neurosurgery, Montreal Neurological Institute, Montreal, Quebec H3A 2B4, Canada;

and ³Department of Biological Sciences, University of Iowa, Iowa City, Iowa 52242

White, John A., Ruby Klink, Angel Alonso, and Alan R. Kay.

Noise from voltage-gated ion channels may influence neuronal dynamics in the entorhinal cortex. *J. Neurophysiol.* 80: 262–269, 1998. Neurons of the superficial medial entorhinal cortex (MEC), which deliver neocortical input to the hippocampus, exhibit intrinsic, subthreshold oscillations with slow dynamics. These intrinsic oscillations, driven by a persistent Na⁺ current and a slow outward current, may help to generate the theta rhythm, a slow rhythm that plays an important role in spatial and declarative learning. Here we show that the number of persistent Na⁺ channels underlying subthreshold oscillations is relatively small ($<10^4$) and use a physiologically based stochastic model to argue that the random behavior of these channels may contribute crucially to cellular-level responses. In acutely isolated MEC neurons under voltage clamp, the mean and variance of the persistent Na⁺ current were used to estimate the single channel conductance and voltage-dependent probability of opening. A hybrid stochastic-deterministic model was built by using voltage-clamp descriptions of the persistent and fast-inactivating Na⁺ conductances, along with the fast and slow K⁺ conductances. All voltage-dependent conductances were represented with nonlinear ordinary differential equations, with the exception of the persistent Na⁺ conductance, which was represented as a population of stochastic ion channels. The model predicts that the probabilistic nature of Na⁺ channels increases the cell's repertoire of qualitative behaviors; although deterministic models at a particular point in parameter space can generate either subthreshold oscillations or phase-locked spikes (but rarely both), models with an appropriate level of channel noise can replicate physiological behavior by generating both patterns of electrical activity for a single set of parameters. Channel noise may contribute to higher order interspike interval statistics seen in vitro with DC current stimulation. Models with channel noise show evidence of spike clustering seen in brain slice experiments, although the effect is apparently not as prominent as seen in experimental results. Channel noise may contribute to cellular responses in vivo as well; the stochastic system has enhanced sensitivity to small periodic stimuli in a form of stochastic resonance that is novel (in that the relevant noise source is intrinsic and voltage-dependent) and potentially physiologically relevant. Although based on a simple model that does not include all known membrane mechanisms of MEC stellate cells, these results nevertheless imply that the stochastic nature of small collections of molecules may have important effects at the cellular and network levels.

INTRODUCTION

Electrical noise plays an important, if poorly understood, role in the functioning of the nervous system. The principal source of this noise is assumed typically to be synaptic, resulting from the probabilistic release of synaptic vesicles.

Contributions of the inherently stochastic nature of voltage-gated ion channels to neuronal noise levels are widely assumed to be minimal because of the large number of channels involved. However, evidence from experimental (Johansson and Århem 1994; Sigworth 1980; Verveen 1961), theoretical (Chow and White 1996; Lecar and Nossal 1971a,b) and computational (Rubinstein 1995; Schneidman et al. 1998; Skaugen and Walløe 1979; Strassberg and DeFelice 1993) studies indicates that noise from voltage-gated channels can have important effects at the cellular level.

The possible importance of intrinsic noise from voltage-gated channels is emphasized by recent results demonstrating that additive noise can allow dramatic improvements in representations of weak signals in neuronal systems (Bezrukov and Vodyanov 1995; Collins et al. 1996; Douglass et al. 1993; Levin and Miller 1996). This result holds for systems of one nonlinear unit and, more dramatically, for systems that sum the responses of parallel units (Collins et al. 1995). If stochastic ion channels are an important neuronal noise source, they may serve to boost responses to weak signals as well.

Here we study the effects of channel noise in neurons of the superficial medial entorhinal cortex (MEC), which are responsible for delivering information from the association cortices to the hippocampus via the perforant path. These neurons exhibit subthreshold oscillations in membrane potential at a frequency of ~ 8 Hz (Alonso and Klink 1993; Alonso and Llinás 1989). The subthreshold oscillations are generated by a mechanism involving a persistent (noninactivating) Na⁺ conductance and a slow outward conductance (Klink and Alonso 1993; White et al. 1995). The persistent Na⁺ conductance is small (White et al. 1995) and, consequently, thought to be mediated by a modest number of ion channels.

The approach used here involves three steps. First, we characterize the population of persistent Na⁺ channels under voltage clamp in acutely isolated cells from the MEC. This characterization gives us a mathematical description of the properties of the channels. Second, we construct a computational model to represent the major populations of ion channels responsible for subthreshold oscillations and spiking behavior. In this model persistent Na⁺ channels are represented as a population of identical stochastic devices with two states (open and closed). Other, larger populations are represented in deterministic Hodgkin-Huxley form. We show that the range of qualitative behaviors that the model

can exhibit depend crucially on the level of channel noise and tune the model to best describe current-clamp results from MEC neurons. Third, we use the tuned model to demonstrate that channel noise may make important contributions to interspike interval statistics and the probability of responding to a weak, physiologically relevant stimulus. Two specific properties of the channel noise—its voltage-dependence and bandwidth—make important contributions to these results.

METHODS

Experimental methods

ISOLATED NERVE CELLS. Isolated cells were studied by using previously published methods (White et al. 1993). Briefly, male rats (125–200 g) were anesthetized with pentobarbital sodium (Nembutal; 30 mg/kg) and decapitated. The brain was quickly removed and a block of tissue containing the retrohippocampal region was cut. Horizontal slices (350 μm) were cut in cold (6–10°C), oxygenated Ringer solution containing (in mM) 115 NaCl, 5 KCl, 1 CaCl₂, 4 MgCl₂, 20 piperazine-*N,N'*-bis(2-ethanesulfonic acid), and 25 glucose. Slices were cut into chunks containing only the superficial MEC. These chunks were transferred to a stir flask, brought to 30°C, reacted with proteinase K (0.2 mg/ml) for 5 min and trypsin (1 mg/ml) for 30 min, and allowed to return to room temperature. Dissociated cells were isolated from the MEC chunks by mechanical trituration. Recordings were made in a solution containing (in mM) 120 NaCl, 5 CsCl, 2 CaCl₂, 2 MgCl₂, 15 tetraethylammonium Cl, 5 4-amino-pyridine, 10 *N*-2-hydroxyethylpiperazine-*N'*-2-ethanesulfonic acid (HEPES), and 25 glucose, pH = 7.4. Voltage-clamp recordings were made by using the whole cell patch technique with an Axopatch 200A amplifier (Axon Instruments). The recording solution contained (in mM) 120 CsF, 15 NaCl, 10 HEPES, and 11 ethylene glycol-bis(β -aminoethyl ether)-*N,N,N',N'*-tetraacetic acid ($R = 1\text{--}3\text{ M}\Omega$). Data were low-pass filtered with a cutoff frequency of 5 kHz and sampled at 20 kHz.

BRAIN SLICES. Horizontal brain slices of the MEC (350 μm) were cut by following previously published methods (Alonso and Klink 1993). Recordings were made in Ringer solution containing (in mM) 124 NaCl, 5 KCl, 1.2 KH₂PO₄, 2.4 CaCl₂, 2.6 MgSO₄, 26 NaHCO₃, and 10 glucose, pH = 7.4 while saturated with 95% O₂-5% CO₂. The rather large value of extracellular K⁺ concentration [K⁺]_o = 6.2 mM was used for continuity with previous work in this system (Alonso and Klink 1993; Alonso and Llinás 1989), but very similar results are obtained with lower concentrations; in fact, the experimental data from Fig. 4 were collected with [K⁺]_o = 3 mM. Layer 2 of the MEC was identified via transillumination. Sharp electrodes, filled with potassium acetate (3 M; $R = 40\text{--}80\text{ M}\Omega$), were used for intracellular current-clamp recordings, which were made with the use of an Axoclamp 2B amplifier (Axon Instruments). Data were low-pass filtered with a cutoff frequency of 1 kHz and sampled at 2.5 kHz.

Modeling methods

The single-compartment model is described by the current-balance equation: $C_m dV_m/dt = -\bar{g}_{\text{Na}1} m^3(V_m) h(V_m, t) [V_m - V_{\text{Na}}] - \bar{g}_{\text{K}1} n^4(V_m, t) [V_m - V_{\text{K}}] - N_o \gamma [V_m - V_{\text{Na}}] / SA - \bar{g}_{\text{K}2} w(V_m, t) [V_m - V_{\text{K}}] - \bar{g}_{\text{L}} [V_m - V_{\text{L}}] + i_{\text{app}}$, where $C_m = 1.5\ \mu\text{F}/\text{cm}^2$, $\bar{g}_{\text{Na}1} = 53\ \text{mS}/\text{cm}^2$, $\bar{g}_{\text{K}1} = 30\ \text{mS}/\text{cm}^2$, $\bar{g}_{\text{L}} = 0.1\ \text{mS}/\text{cm}^2$, N_o = the number of open persistent Na⁺ channels, γ = the single-channel conductance of the persistent Na⁺ channel, SA = cellular surface area, $V_{\text{Na}} = 55\ \text{mV}$, $V_{\text{K}} = -69\ \text{mV}$, and $V_{\text{L}} = -54\ \text{mV}$. [The value of C_m used is slightly larger than recent results (Major et al. 1994)

would indicate, but is compatible with estimates we have made in the past (White 1990) and with the notion that our rough estimates of surface area are low because they neglect the effects of enfolding. In any event, inaccuracies in the value of C_m can be offset by scaling conductance values in the current-balance equation.] In tuning the model to match experimental data, $\bar{g}_{\text{K}2}$ was varied between 8.5–13 mS/cm²; $\bar{g}_{\text{Na}2} = \gamma p_0 N / SA$ (where p_0 and N are the maximal probability of opening and number of persistent Na⁺ channels, respectively) was varied from 0.15–0.3125 mS/cm². Changes in N or $\bar{g}_{\text{Na}2}$ were made independent of other parameters by altering surface area SA. By keeping all other aspects of the model the same, this method allowed us to examine the effects of these changes in a well-controlled manner. Each of the deterministic gating variables (m , h , n) is described by a first-order, nonlinear ordinary differential equation (ODE) of Hodgkin-Huxley form. Mathematical descriptions of gating variables and other parameters were derived from voltage-clamp data from isolated cells (Eder et al. 1991; White et al. 1993, 1995).

Stochastic persistent Na⁺ channels were modeled with the use of a previously published method (Chow and White 1996) that relies on the joint probability distribution of any state transition in a system of N identical, independent ion channels. We used a simple two-state Markov process model of the persistent Na⁺ channels not because we believe it to be correct—persistent Na⁺ currents undoubtedly arise via complex ion channel kinetics (e.g., Alzheimer et al. 1993)—but rather because it was the simplest model that fit the available voltage-clamp data, matching the mean and coefficient of variation (the ratio of SD to mean) of the steady-state, tetrodotoxin (TTX)-sensitive Na⁺ current within the relevant range of membrane potentials. An activation time constant $\tau = 0.15\ \text{ms}$ was used for the persistent current to match the high (>1 kHz) bandwidth of this current (Fig. 1C).

Data analysis

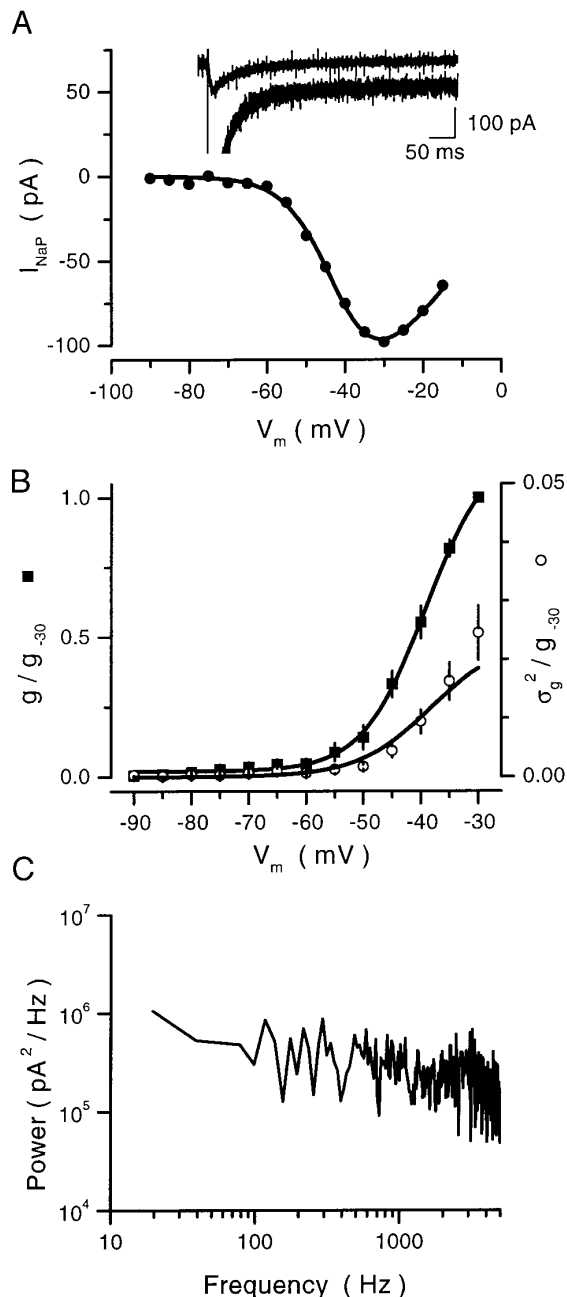
COUNTING CHANNELS. The procedure for characterizing an assumed homogeneous population of ion channels is based on a binomial model in which the mean conductance $g(V_m) = N\gamma p(V_m)$, where N is the number of channels in the population, γ is the single-channel conductance, and $p(V_m)$ is the voltage-dependent probability that each channel is open. Under this model the variance of conductance, also voltage-dependent, is given by the equation $\sigma_g^2(V_m) = N\gamma^2 p(V_m) [1 - p(V_m)]$. $p(V_m)$ can be parameterized by the function $p(V_m) = p_0 f(V_m)$, where p_0 is the maximal probability of opening of the channel and $f(V_m) = 1/[1 + \exp(-(V_m - V_0)/dV)]$ is a Boltzmann function. Under ideal conditions one would use these two relationships, along with measurements of g and σ_g over the entire range of relevant potentials, to estimate N , γ , and the form of $p(V_m)$. In our case the diminutive size of the persistent Na⁺ conductance left us with reliable data only for potentials less than or equal to $-30\ \text{mV}$. We estimated N , γ , p_0 , V_0 , and dV by using a multistep process. First, we divided mean and variance data by the value of g at $-30\ \text{mV}$ to allow comparison among different cells (Fig. 1B). This normalization procedure is equivalent to multiplying each by a factor $\alpha = [N\gamma p_0 f(-30)]^{-1}$. Normalized mean and variance data were fit simultaneously by using the functions $\beta\gamma p_0 f(V_m)$ and $\beta\gamma^2 p_0 f(V_m) [1 - p_0 f(V_m)]$, respectively, where $\beta = \alpha N$. Values of the parameters γ and p_0 were searched over discrete spaces with mesh size 5 pS and 0.05, respectively. Once the values of β , γ , p_0 , V_0 , and dV were determined from the lumped data, the estimated value of N for each cell was determined from the relationship $n = \beta/\alpha$. Channel counts from isolated cells were taken only as preliminary estimates that were refined by fitting the bifurcation and power-spectral properties of current-clamp recordings from MEC cells in brain slices.

ANALYZING SPIKE CLUSTERS. Clustering was analyzed in sequences of interspike intervals, calculated off-line from digitized

data. A cluster of M spikes was defined by the presence of $M-1$ adjacent intervals of length $0.5-1.5 T$, where T is the period of underlying subthreshold oscillations, determined from the fast Fourier transform (FFT) power spectrum. Isolated action potentials were considered clusters of length $M = 1$. The probability of observing a cluster of length M [$p(M)$] was estimated by dividing the number of observed clusters of length M by the total number of clusters in the data set.

RESULTS

We studied the persistent Na^+ conductance under whole cell voltage clamp in dissociated MEC neurons. Figure 1A, *inset*, shows voltage-clamp responses (prepulse potential = -90 mV, pulse potential = -40 mV) in the presence (*top trace*) and absence (*bottom trace*) of $1 \mu\text{M}$ TTX. In the



absence of TTX, the major membrane current is a large, fast Na^+ current (clipped in this trace) that settles to a persistent value of approximately -70 pA. In TTX both the fast and persistent Na^+ currents are blocked, leaving only a transient inward current (probably carried by Ca^{2+} , but not studied in detail).

The points in Fig. 1A show the current-voltage relationship for the persistent Na^+ current, derived from voltage-clamp responses by subtracting records in $1 \mu\text{M}$ TTX from control records and averaging over the last 200 ms of the subtracted record. The solid line shows a least-squares fit of a Boltzmann function-driving force product to the data.

For membrane potentials between -60 and -35 mV and with other conductances blocked, the Na^+ -channel mediated component is responsible for the great majority of the mean and as much as 80% of the variance in total recorded current (e.g., compare the means and variances of the *top* and *bottom* traces in Fig. 1A, *inset*). The steady-state mean and variance of the persistent Na^+ conductance are shown for several cells over a range of clamp potentials in Fig. 1B. To allow comparisons among cells, both means and variances have been normalized by the mean value of the conductance at $V_m = -30$ mV (see METHODS). Using these values and a binomial modeling method we estimated the number of channels N , single-channel conductance γ , maximum probability of opening p_0 , half-activation point V_0 , and steepness of the activation function dV . From this procedure we obtained the following estimates: $\gamma = 20$ pS, $p_0 = 0.125$, $V_0 = -37.5$ mV, and $dV = 6.5$ mV. The estimated value of N ranged from 388 to 2,498 with a mean value of 1,276 ($n = 4$). In this paper we take the values of γ , p_0 , V_0 , and dV as set, but recalibrate the value of N for cells in brain slices, which contain more of their processes and thus potentially more Na^+ channels, by matching current-clamp data (see Fig. 3).

The frequency content of the TTX-sensitive persistent Na^+ current was examined by taking FFTs of subtracted traces. Figure 1C shows the power spectrum from the last 200 ms of the difference between the current traces in Fig. 1A, *inset*. As exemplified by this trace, power spectra were consistently flat (or in some cases, displayed possible $1/f^\alpha$ behavior) for frequencies $< 1-3$ kHz. Bandwidth limitations

FIG. 1. Estimating single-channel characteristics from macroscopic data in isolated cells. *A*: persistent Na^+ current (I_{NaP}) isolated in a dissociated neuron from the superficial medial entorhinal cortex by subtracting steady-state responses in $1 \mu\text{M}$ tetrodotoxin (TTX) from those under control conditions. Voltage clamp protocol involved a long (500 ms) step to a voltage potential V_m from a holding potential of -90 mV. *Inset*: sample recordings in TTX and under control conditions with $V_m = -40$ mV. Prepulse currents have mean \pm SD of -0.8 ± 9.6 pA (control) and 0.1 ± 6.5 pA (TTX). Steady-state responses (last 200 ms of each trace) have -74.7 ± 12 pA (SD; control) and -0.02 ± 6.5 pA (TTX). Data points in the main panel are mean values of steady-state current at different clamp potentials. Smooth curve, least-squares fit of a Boltzmann function (with driving force included) to the data. *B*: symbols are normalized mean conductance (g/g_{-30} , closed) and variance of conductance (σ_g^2/g_{-30} , open) [$n = 4$ (SE)] plotted vs. V_m . Solid curves, results of simultaneous least-squares fit to the experimental data by using a binomial model (see METHODS). *C*: power spectrum of the persistent Na^+ current. The trace was obtained by taking the difference between the traces in *panel A inset* and taking the fast Fourier transform (FFT) of these data under steady-state conditions (i.e., for the last 200 ms of the command pulse; see METHODS). The point at 60 Hz has been deleted from the plot.

of our recordings prevent us from knowing the cutoff frequency f_0 of these records, but in all cases examined this cutoff was ≥ 1 kHz, implying that the activation time constant $\tau = 1/(2\pi f_0)$ of the persistent Na^+ channels is ≤ 0.16 ms.

Because the population of persistent Na^+ channels [or alternatively, the population of Na^+ channels that are in the persistent “mode” (Alzheimer et al. 1993)] contributes significantly to total membrane noise, it stands to reason that the electrical noise induced by a flicker of the probabilistic channels may have an effect on macroscopically measured oscillations. To test this hypothesis we constructed a model of sub- and suprathreshold behavior in MEC cells. The model consisted of a membrane capacitance in parallel with a leak conductance and four nonlinear conductances (see METHODS). Two of the nonlinear conductances—the persistent Na^+ current and a slow K^+ current—generate subthreshold oscillations. The remaining two—a fast, inactivating Na^+ current and a delayed rectifier—underlie action potentials. The model differs from typical models of excitable membranes in that the persistent Na^+ conductance is modeled not with deterministic, nonlinear differential equations but rather as a set of two-state (open and closed) Markov processes. The parameters of this Markov model were chosen to mimic the most fundamental and consistent features of the persistent Na^+ channels (specifically, the mean and variance of the steady-state current-voltage relationship, as well as the broadband nature of the channel noise). The remaining three active conductances are 2–3 orders of magnitude larger than $g_{\text{Na}2}$, implying that they can be modeled sufficiently by using deterministic methods.

Figure 2 shows maps of this qualitative behavior as a function of the maximal magnitudes of the persistent Na^+ conductance ($\bar{g}_{\text{Na}2} = \gamma p_0 N / SA$) and slow potassium conductance ($\bar{g}_{\text{K}2}$) for the following three model types: deterministic, stochastic with $n = 1,200$, and stochastic with $N =$

4,800. The five shades, labeled as Regions 1–5 at the right, represent regions of qualitative behavior for stimulation over a large range of positive DC currents. From *bottom right* to *top left*, Region 1 represents models that are silent for all levels of current injection; Region 2, models that are quiet at rest and generate subthreshold oscillations but no spikes with positive DC current; Region 3, models that generate quiescence, subthreshold oscillations, and spikes, replicating results from intracellular recordings; Region 4, models that exhibit quiescence and spikes but no subthreshold oscillations; and Region 5, models that spike spontaneously.

The three model types show significant differences in qualitative behavior. The map for deterministic models is dominated by the quiescent (Region 1) and spiking (Regions 4 and 5) regions. The map for stochastic models with $N = 1,200$ is dominated by Regions 1, 2, and 5. This model type shows more excitability than the deterministic model, but again Region 3 is sparsely represented. The map for stochastic models with $N = 4,800$ shows all five regions. Most importantly, it is the only map of the three that reliably mimics the cells’ ability to generate spikes, subthreshold oscillations, and phase-locked spikes without an exotic mechanism involving current-dependent modulation of maximal conductance values. We take this as evidence that $N \approx 4,800$ in intact cells. The fact that this estimate is higher than estimates obtained from isolated cells may reflect the fact that in the isolation procedure, the cell loses most of even its most proximal processes and hence some fraction of its voltage-gated ion channels.

We determined best-fit values of $\bar{g}_{\text{Na}2}$, $\bar{g}_{\text{K}2}$, and N for further analysis by searching systematically through this parameter space and matching power spectra at a given level of depolarization to those from experimental results. Figure 3, A–B, shows examples from this analysis with $\bar{g}_{\text{Na}2} = 0.25$ mS/cm² and $\bar{g}_{\text{K}2} = 10.6$ mS/cm². Plotted are results with varying N in the time (A) and frequency (B) domains. As

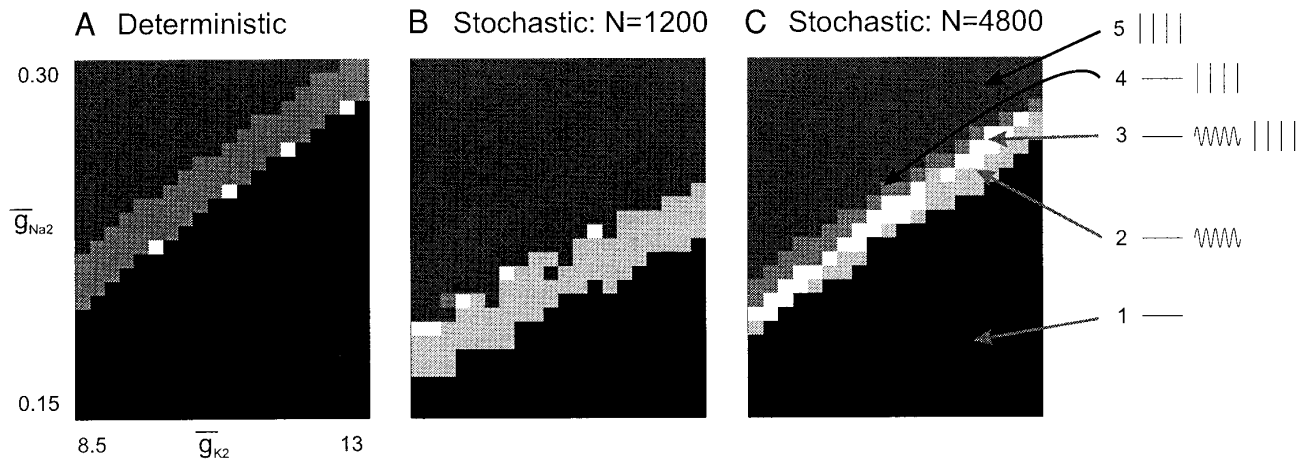


FIG. 2. Channel noise affects qualitative behavior. Shown are maps of qualitative behavior as a function of the maximal values of the persistent Na^+ conductance ($\bar{g}_{\text{Na}2}$) and slow K^+ conductance ($\bar{g}_{\text{K}2}$) for 3 model types. Changes in $\bar{g}_{\text{Na}2}$ or N were effected by changing the size of the membrane area that was simulated, thus leaving all other aspects of the model unchanged. Behavior was mapped by applying currents from 0–3 $\mu\text{A}/\text{cm}^2$ and measuring the ratio of AC to total power and the probability of spike generation per subthreshold cycle. The AC power ratio threshold for subthreshold oscillations was 1.4×10^{-4} , equivalent to a 1-mV sinusoid superimposed on a membrane potential of -60 mV. The threshold for reliable spiking was a probability of 0.1/cycle. Shade-coded regions, numerically identified to the right of *panel C*, represent different combinations of quiescent, subthreshold oscillatory and spiking behavior over the current range tested and are explained in the text.

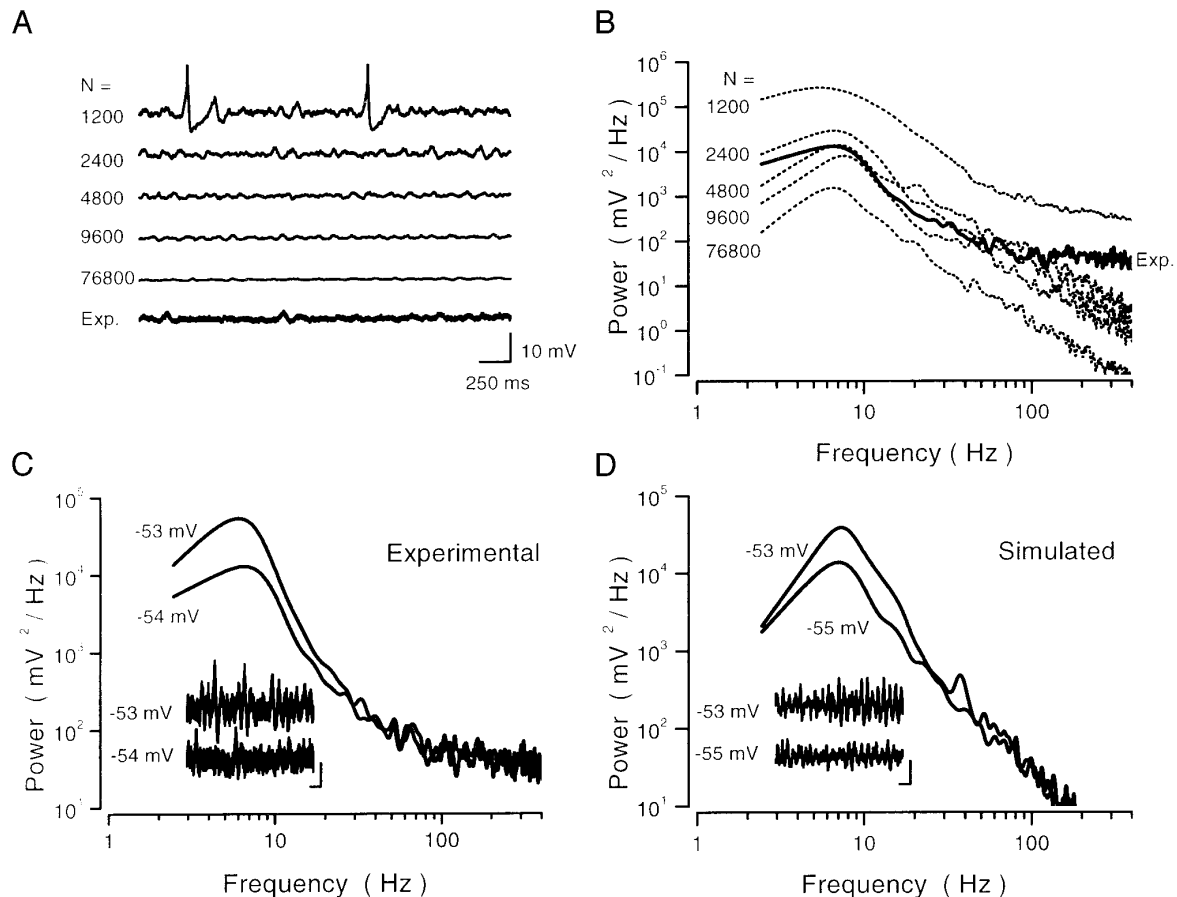


FIG. 3. Matching simulated responses to recorded results. *A, top traces*: simulated responses to modest depolarization with different numbers of persistent Na^+ channels. In these and all simulated results in Figs. 3–5, we took $\bar{g}_{\text{Na}2} = 0.25 \text{ mS/cm}^2$ and $\bar{g}_{\text{K}2} = 10.6 \text{ mS/cm}^2$. *A, bottom trace*: recorded response at a similar level of depolarization ($\sim -54 \text{ mV}$). Exp, experimental. *B, dotted traces*: power spectra of traces in *panel A*, in the same order from *top to bottom*. *B, solid trace*: power spectrum from the recorded trace. Spectra are the average power from a series of 14 short-time, 1,024-point FFTs, calculated from a data trace of duration 3 s. Data windows were shifted 512 points for each iteration of the short FFT. For each data segment the mean potential was subtracted away and a Hamming window was applied. *C, inset*: recorded responses for 2 levels of mean potential (-54 mV , *bottom trace*; -53 mV , *top trace*) in a neuron from layer 2 of the medial entorhinal cortex (MEC). Horizontal scale, 250 ms; vertical scale, 1 mV. *C, main plot*: power spectra generated from signals shown in the *inset*. Methods as described in *panel B*. *D, inset*: simulated responses from stochastic model with 4,800 persistent Na^+ channels and mean potentials of -55 mV (*bottom trace*) and -53 mV (*top trace*). Scales, see *panel C, inset*. *D, main Plot*: power spectra of the simulated responses. Methods as described for *panel B*.

N increases, the simulated response becomes less energetic, approaching the quiescent behavior of the related deterministic system at this level of depolarization. The $N = 4,800$ case matches the experimental results for this and higher (Fig. 3, *C–D*) levels of depolarization. Experimental and simulated results match well in peak power, peak frequency, and high-frequency slope, differing mainly in that the experimental data exhibit a noise floor at high frequencies and more low-frequency energy. Below, we use these values of $\bar{g}_{\text{Na}2}$, $\bar{g}_{\text{K}2}$, and N exclusively.

If depolarized sufficiently, MEC stellate cells and our stochastic model exhibit action potentials that rise from the depolarizing phase of the subthreshold oscillations. As exemplified by the traces of Fig. 4*A*, these action potentials do not occur randomly but rather in distinct “spike clusters” (i.e., on ≥ 2 adjacent cycles). Spike clustering can be quantified by measuring the probability of observing a spike cluster of M spikes ($M = 1, 2, 3, \dots$). Figure 4*B* shows a plot of $p(M)$ versus M for experimental data (solid symbols) and

simulations with channel noise (open symbols). Also shown is the expected value of $p(M)$ for a “memoryless” process with the same probability of spiking per cycle (0.22) but with no dependence of spiking probability on past history. Models with channel noise show evidence of spike clustering, in the form of enhanced $p(M)$ for $M > 1$. This effect does not depend critically on the bandwidth of the channel noise; increasing the activation time constant of the persistent Na^+ channels to a value 5 times slower than we estimated above has only mild effects on clustering (open triangles; we believe the differences seen between the open circles and open triangles are due to necessary changes in mean V_m necessary to control for spiking probabilities in these 2 models). Spike clustering appears strongest in experimental data, for which clusters of length $M = 2$ are most probable, although limitations in the amount of data make this conclusion less than firm. If real, this preponderance of clusters of length $M = 2$ in the experimental results may be due to rebound spikes not accounted for in our model or other,

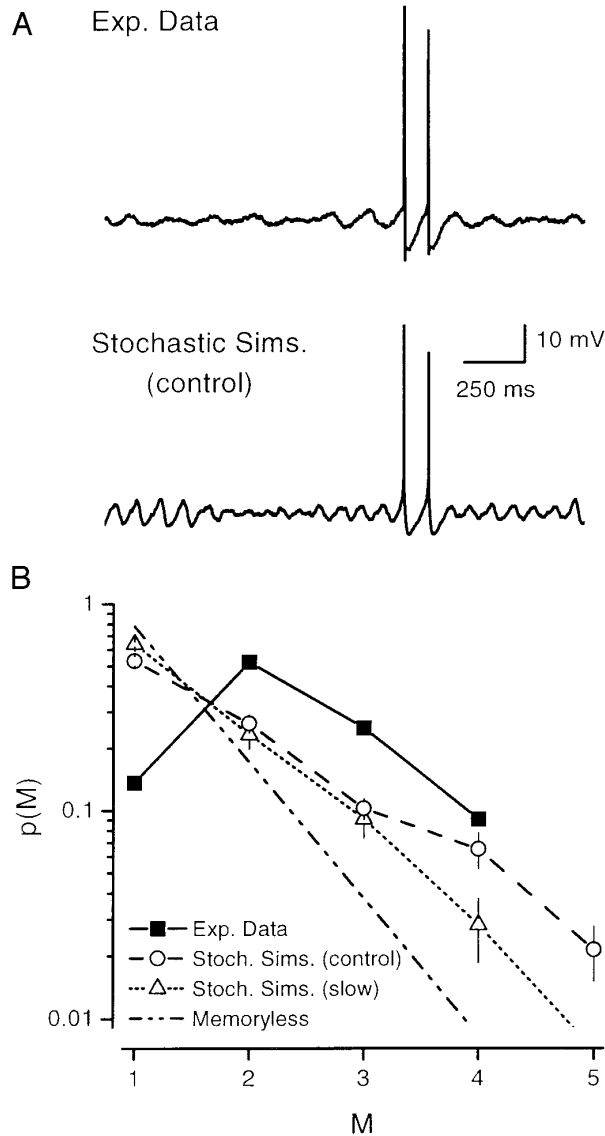


FIG. 4. Models incorporating channel noise mimic some, but not all, interspike interval characteristics of MEC stellate cells. *A*: example traces for experimental (*top*) and simulated (*bottom*) results. Spike clustering is seen in both cases. *B*: $p(M)$, the probability of a spike cluster of length M , plotted vs. M for experimental data, as well as channel-noise simulations with control ($\tau = 0.15$ ms) and slow ($\tau = 0.75$ ms) values of the persistent Na^+ channels' activation time constant. Values for the stochastic simulations (stoch. sims.) are mean \pm SD ($n = 4$; $\sim 1,200$ intervals total). Values for experimental data are based on analysis of 102 intervals. Also shown is the expected value of $p(M)$ for a "memoryless" model (i.e., predicted response of a model in which probability of spike generation per cycle of the subthreshold oscillation is independent of past events). All experimental and simulated data have the same estimated probability of spiking per cycle.

more complex dynamical influences (Rush and Rinzel 1995; Wang 1993).

Under in vivo conditions in the theta state, cells of the MEC are driven at theta frequencies by their peers and respond in phase with the input stimulus. Results from Fig. 2 show that channel noise increases excitability, pointing to the possibility that MEC neurons may use channel noise to enhance their responses to weak periodic stimuli in a form of stochastic resonance. We examined this possibility by comparing responses of deterministic and stochastic models

to periodic excitatory input. Under modeled conditions the deterministic model jumps from a purely subthreshold response (Fig. 5*A*, *left-middle trace*) to a 3.5-Hz doublet response (*left-top*) over a narrow range of input conductance magnitudes (Fig. 5*B*, solid line). A continued increase in the magnitude of the synaptic conductance drives the system to respond every cycle of the 7-Hz input.

The stochastic model behaves quantitatively and qualitatively differently. Channel noise renders this model more sensitive to small stimuli (Fig. 5). For the control model (Fig. 5*A*, *right traces*; Fig. 5*B*, dashed line) with rapid persistent Na^+ channels, the probability of a response per cycle remains higher than that of the deterministic model for nearly all values of g_{syn} , and responses are nearly always

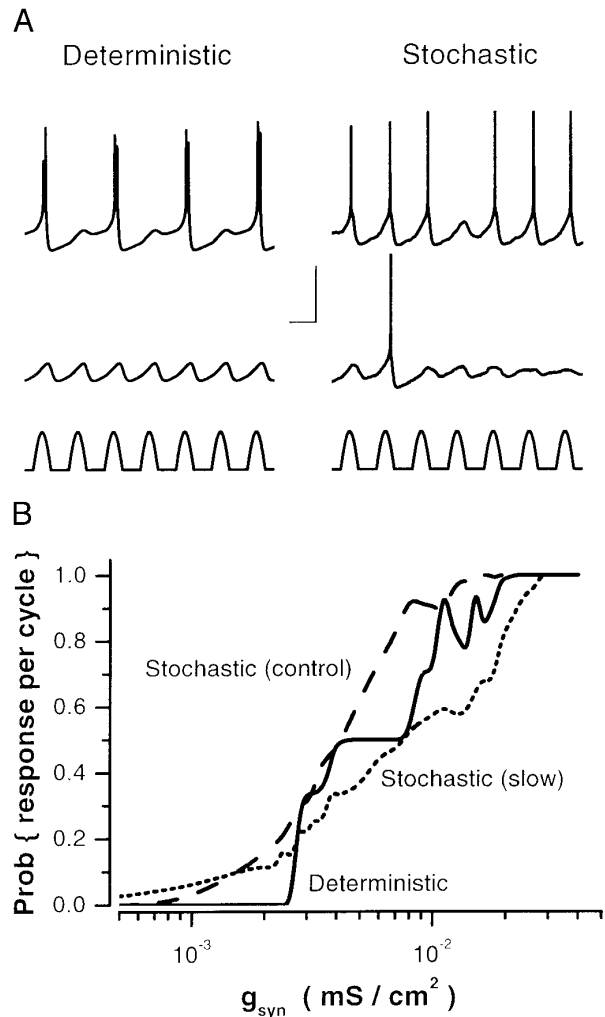


FIG. 5. Models with channel noise exhibit increased sensitivity to weak periodic stimuli. *A*, *bottom traces*: half-wave rectified, excitatory synaptic input ($V_{\text{syn}} = 0$ mV), delivered to deterministic (*left side*) and stochastic (*right side*) models of MEC cells. *Middle traces*: responses with $g_{\text{syn}} = 2 \mu\text{S}/\text{cm}^2$. *Top traces*: responses with $g_{\text{syn}} = 6 \mu\text{S}/\text{cm}^2$. Stochastic models fire doublets much less often but give an enhanced probability of firing per cycle. *B*: summary results for deterministic and 2 stochastic models—one with control value (0.15 ms) of the persistent Na^+ channels' activation time constant and one that activates 5 times more slowly. Both stochastic models give an enhanced probability of firing for low g_{syn} . They differ in their behavior for high g_{syn} . Response of the deterministic model is unaltered by this manipulation.

single spikes rather than doublets. (Stochastic models do show doublets reliably for nearby regions of parameter space.) In contrast to spike-clustering results with DC stimulation (Fig. 4), response probabilities to AC stimulation depend on the bandwidth of the channel noise. Slowing down the activation time constant of the persistent Na^+ channels by a factor of 5 (Fig. 5B, dotted lines) gives an enhanced probability of response only for small values of g_{syn} . This manipulation has no effect on the underlying deterministic system (data not shown), indicating that the difference between the dashed and dotted lines in Fig. 5B is a property of channel-noise bandwidth rather than one of the related deterministic dynamics.

DISCUSSION

In our simulations two factors make channel noise an important contributor to cellular response properties in the MEC. First, a relatively small number of persistent Na^+ channels gives a relatively high coefficient of variation (CV; the ratio of SD to mean is proportional to $N^{-1/2}$) in induced current. Second, this conductance is strategically positioned (via its activation properties and associated reversal potential) so that its activation drives the cell from near resting potential to spike threshold. Together, these factors make many of the general effects of channel noise rather insensitive changes in the specific form of the noise; changing the threshold (data not shown), bandwidth (Figs. 4–5), or voltage dependence (data not shown) of the noise altered the details but not the basic properties of our results. This robustness lies in the simple fact that the amount of channel noise we measure directly (Fig. 1) is sufficient to deflect the trajectory of the voltage signal as it traces a path in phase space. Because the effects of channel noise are robust, we expect such effects to be significant in many nerve cells that exhibit persistent Na^+ conductances (Llinás 1988), as well as in other neurons without prominent persistent Na^+ currents (Chow and White 1996; Johansson and Århem 1994; Lecar and Nossal 1971a,b; Rubinstein 1995; Schneidman et al. 1998; Sigworth 1980; Skaugen and Walløe 1979; Strassberg and DeFelice 1993; Verveen 1961). Effects of the kind we describe may be important more generally, as exemplified by recent work implicating stochastic chemical reactions in other nonlinear physiological systems, including retinal transduction (Felber et al. 1996) and regulation of gene expression (McAdams and Arkin 1997).

Among the putative effects of channel noise reported here is a form of stochastic resonance (SR) with weak periodic stimuli. The noise source underlying this effect differs from that used in other neuronal studies (Collins et al. 1996; Douglass et al. 1993; Levin and Miller 1996) in two ways. First, the noise source in our case is an intrinsic characteristic of the system rather than experimentally imposed. Thus rather than relying on the input's having an appropriate level of noise to boost but not overwhelm pertinent weak inputs, the cell has the opportunity to modify its noise level dynamically. Second, the level of channel noise in MEC neurons is voltage dependent and thus covaries with the level of excitation. This voltage dependence has demonstrable effects on the model's behavior; although the stochastic simulation results of Fig. 4 can be replicated by a deterministic

model with additive, voltage-independent noise, spike clustering at lower spiking probabilities occurs only with simulated channel noise and not with voltage-independent noise (data not shown). The voltage dependence of channel noise may contribute to the results of Fig. 5 as well.

Subject to the caveat that our model leaves out known nonlinear properties of MEC stellate cells (e.g., the slow inward rectifier), our results suggest that the precise channel numbers are relevant not only for determining neuronal reliability and threshold but also for the qualitative form of dynamics expressed by the neuron. For example, the maps of Fig. 2 show that the level of channel noise can determine the number of qualitative states that an excitable cell can enter; unlike its counterparts, the stochastic family of models with $N = 4,800$ can generate physiologically relevant Region 3 behavior robustly. This result implies that mismatches between the dynamics of deterministic models and actual neuronal response in some cases may result not from any inaccuracies in the model, but rather from a failure to incorporate the effects of stochastic channel gating. In stellate neurons of the MEC, noise induced by channel flicker is large enough to alter cellular input-output properties in response to both constant and time-varying stimuli. If this effect is indeed important, the statistical properties of voltage-gated ion channels may exert an effect on the dynamics of neuronal networks.

We thank C. Chow, J. Collins, J. Rinzel, and A. Sherman for valuable discussions and F. Moss for reading an earlier version of this manuscript. Some of the current-clamp data were collected and shared graciously by B. Haman.

This work was supported by grants from the National Institutes of Health and the Whitaker Foundation to J. A. White, the Medical Research Council to A. Alonso, and the National Institute of Neurological Disorders and Stroke and the Office of Naval Research to A. R. Kay.

Address reprint requests to: J. A. White, Dept. of Biomedical Engineering, Boston University, 44 Cummington St., Boston, MA 02215.

Received 20 November 1997; accepted in final form 30 March 1998.

REFERENCES

- ALONSO, A. AND KLINK, R. M. Differential electroresponsiveness of stellate and pyramidal-like cells of medial entorhinal cortex layer II. *J. Neurophysiol.* 70: 128–143, 1993.
- ALONSO, A. AND LLINÁS, R. R. Subthreshold Na^+ -dependent theta-like rhythmicity in stellate cells of entorhinal cortex layer II. *Nature* 342: 175–177, 1989.
- ALZHEIMER, C., SCHWINDT, P. C., AND CRILL, W. E. Modal gating of Na^+ channels as a mechanism of persistent Na^+ current in pyramidal neurons from rat and cat sensorimotor cortex. *J. Neurosci.* 13: 660–673, 1993.
- BEZRUKOV, S. M. AND VODYANOV, I. Noise-induced enhancement of signal transduction across voltage-dependent ion channels. *Nature* 378: 362–364, 1995.
- CHOW, C. C. AND WHITE, J. A. Spontaneous action potentials due to channel fluctuations. *Biophys. J.* 71: 3013–3021, 1996.
- COLLINS, J. J., CHOW, C. C., AND IMHOFF, T. T. Stochastic resonance without tuning. *Nature* 376: 236–238, 1995.
- COLLINS, J. J., IMHOFF, T. T., AND GRIGG, P. Noise-enhanced information transmission in rat SA1 cutaneous mechanoreceptors via aperiodic stochastic resonance. *J. Neurophysiol.* 76: 642–645, 1996.
- DOUGLASS, J. K., WILKENS, L., PANTAZELOU, E., AND MOSS, F. Noise enhancement of information transfer in crayfish mechanoreceptors by stochastic resonance. *Nature* 365: 337–340, 1993.
- EDER, C., FICKER, E., GÜNDEL, J., AND HEINEMANN, U. Outward currents in rat entorhinal cortex stellate cells studied with conventional and perforated patch recordings. *Eur. J. Neurosci.* 3: 1271–1280, 1991.
- FELBER, S., BREUER, H. P., PETRUCCIONE, F., HONERKAMP, J., AND HOF-

- MANN, K. P. Stochastic simulation of the transducin GTPase cycle. *Biophys. J.* 71: 3051–3063, 1996.
- JOHANSSON, S. AND ÅRHEM, P. Single-channel currents trigger action potentials in small cultured hippocampal neurons. *Proc. Natl. Acad. Sci. USA* 91: 1761–1765, 1994.
- KLINK, R. M. AND ALONSO, A. Ionic mechanisms for the subthreshold oscillations and differential electroresponsiveness of medial entorhinal cortex layer II neurons. *J. Neurophysiol.* 70: 144–157, 1993.
- LECAR, H. AND NOSSAL, R. Theory of threshold fluctuations in nerves. I. Relationships between electrical noise and fluctuations in axon firing. *Biophys. J.* 11: 1048–1067, 1971a.
- LECAR, H. AND NOSSAL, R. Theory of threshold fluctuations in nerves. II. Analysis of various sources of membrane noise. *Biophys. J.* 11: 1068–1084, 1971b.
- LEVIN, J. E. AND MILLER, J. P. Broadband neural encoding in the cricket cercal sensory system enhanced by stochastic resonance. *Nature* 380: 165–168, 1996.
- LLINÁS, R. R. The intrinsic electrophysiological properties of mammalian neurons: insights into central nervous system function. *Science* 242: 1654–1664, 1988.
- MAJOR, G., LARKMAN, A. U., JONAS, P., SAKMANN, B., AND JACK, J.J.B. Detailed passive cable properties of whole-cell recorded CA3 pyramidal neurons in rat hippocampal slices. *J. Neurosci.* 14: 4613–4638, 1994.
- MCADAMS, H. H. AND ARKIN, A. Stochastic mechanisms in gene expression. *Proc. Natl. Acad. Sci. USA* 94: 814–819, 1997.
- RUBINSTEIN, J. T. Threshold fluctuations in an N sodium channel model of the node of Ranvier. *Biophys. J.* 68: 779–785, 1995.
- RUSH, M. E. AND RINZEL, J. The potassium A-current, low firing rates and rebound excitation in Hodgkin-Huxley models. *Bull. Math. Biol.* 57: 899–929, 1995.
- SCHNEIDMAN, E., FREEDMAN, B., AND SEGEV, I. Ion channel stochasticity may be critical in determining the reliability and precision of spike timing. *Neural Comput.* In press.
- SIGWORTH, F. J. The variance of sodium current fluctuations at the node of Ranvier. *J. Physiol. (Lond.)* 307: 97–129, 1980.
- SKAUGEN, E. AND WALLØE, L. Firing behavior in a stochastic nerve membrane model based upon the Hodgkin-Huxley equations. *Acta Physiol. Scand.* 107: 343–363, 1979.
- STRASSBERG, A. F. AND DEFELICE, L. J. Limitations of the Hodgkin-Huxley formalism: effects of single channel kinetics on transmembrane voltage dynamics. *Neural Comput.* 5: 843–855, 1993.
- VERVEEN, A. *Fluctuations in Excitability*. Amsterdam: Drukkerij Holland N. V., 1961.
- WANG, X.-J. Ionic basis for intrinsic 40 Hz neuronal oscillations. *Neuroreport* 5: 221–224, 1993.
- WHITE, J. A. *Electrotonic Models of Stellate Cells of the Ventral Cochlear Nucleus* (PhD Dissertation). Baltimore, MD: The Johns Hopkins Univ., 1990.
- WHITE, J. A., ALONSO, A., AND KAY, A. R. A heart-like Na⁺ current in the medial entorhinal cortex. *Neuron* 11: 1037–1047, 1993.
- WHITE, J. A., BUDDE, T., AND KAY, A. R. A bifurcation analysis of neuronal subthreshold oscillations. *Biophys. J.* 69: 1203–1217, 1995.